JOURNAL OF MATERIALS SCIENCE 23 (1988) 4273–4281

Effects of cooling rate on the shape memory effect thermodynamics of NiTi

A. P. JARDINE*, K. H. G. ASHBEE‡
H. H. Wills Physics Laboratory, University of Bristol, Tyndall Avenue, Bristol BS8 1TL, UK
M. J. BASSETT
British Gas plc, Research and Development Divison, Watson House, Peterborough Road, London SW6 3HN, UK

The cooling rate of near-stoichiometric NiTi after annealing at 500° C is shown to have dramatic effects on the transformation thermodynamics. The slower the rate of cooling, the higher the transformation temperatures with less rhombohedral phase (R-phase) observed in room-temperature X-ray diffraction spectra. Given that this effect is due to the amount of time spent at intermediate temperatures, i.e an ageing effect, calorimetric analysis of specimens aged at 400 or 450° C revealed progressively higher transformation temperatures and latent heats with ageing. These observations are associated with the evolution of a secondary first-order transformation to the R-phase. Analysis of stress–strain data of near-stoichiometric NiTi helices, water quenched from its secondary anneal at 500° C, indicated that a Carnot efficiency of 16% can be expected, compared with 13.5% for the same material when furnace cooled.

1. Introduction

An important practical consideration when employing shape memory effect (SME) alloys as working elements in heat engines or as thermal sensors is reproducibility of the shape memory behaviour. In the case of the intermetallic compound NiTi, for example, it is known that the appearance of a rhombohedral (R) phase is accompanied by lowering of the SME transformation temperature. In its simplest manifestation, SME behaviour owes its origin to the fact that, below the transformation temperature, the alloy is of low crystal symmetry and can be easily plastically deformed by way of growth of some pseudo-twin orientations at the expense of others. To transform martensitically to its higher symmetry high-temperature (B2) crystal structure, the distribution of individuals atoms and hence of different pseudo-twin orientations must first be returned to that which existed before plastic deformation. That is, growth of the twins which grew is reversed and the plastic strain accommodated by twin growth is recovered. In NiTi the complication of a low symmetry phase (R) other than the truly martensitic (B19) phase introduces the possibility of SME behaviour associated with transformation between each low-temperature phase and the high-temperature phase and even, if it occurs, with transformation between the low-temperature phases themselves. Bearing in mind that the so-called SME transformation actually involves four transformation temperatures, i.e. A_s, A_f, M_s and M_f, it is evident that as many as twelve characteristic temperatures may be involved in the SME transformation of NiTi.

The transformation temperature range is strongly affected by the concentration of nickel present [1]. Non-chemical factors which also affect it are the degree of order [2], ageing effects such as precipitation of different phase material [3], and the introduction of dislocations through cold-working, incomplete transformations [4] and thermal cycling through the transformation [5].

To observe the R-phase in stoichiometric NiTi it is necessary to lower the martensite transformation temperature so that the two transformations do not overlap in temperature. Factors which allow this to occur are increasing nickel content [6], annealing at 400° C after cold working [7] and thermal cycling [5]. As these factors are similar to those reported above, the R-phase itself may have an influence on SME behaviour.

Precipitation does not occur in stoichiometric NiTi [8], but has been observed in alloys with an excess of nickel as low as 50.6%. In these off-stoichiometric alloys, ageing effects become important. Suburi *et al.* [3] found that nickel-rich NiTi (Ni > 50.7 at %) was sensitive to heat treatment, in that with ageing at temperatures below 500° C all transformation temperatures increased. This is due to the creation of fine precipitates by ageing. The effect of precipitation of a nickel-rich phase on ageing causes enrichment of titanium in the matrix phase, raising the transformation temperature. In the matrix phase surrounding the precipitates, 1/3(1 1 0) reflections associated with the R-phase were observed. No ageing effects were observed in 50.1 at % Ni–Ti.

* *Present address*: Department of Materials Science, Cornell University, Ithaca, New York 14853, USA.
‡ *Present address*: Department of Materials Science, University of Tennessee, Knoxville, Tennessee, USA.

0022–2461/88 $03.00 + .12

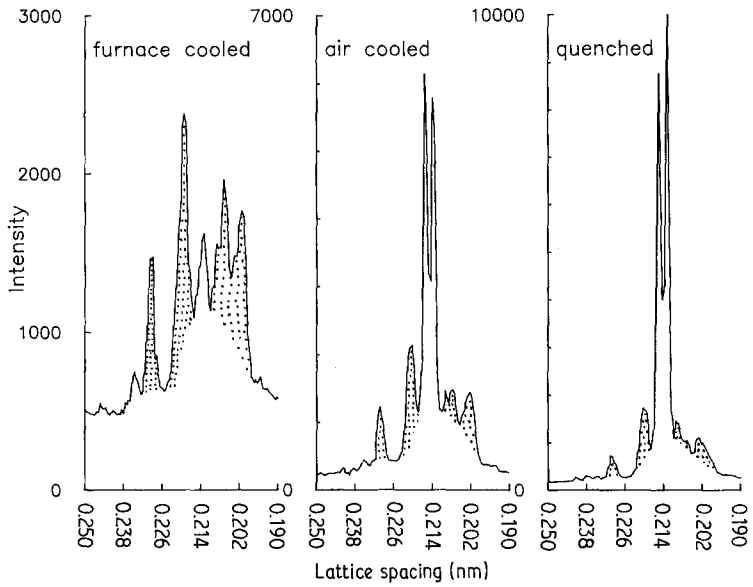

Figure 1 X-ray diffraction spectra for a sample at various cooling rates. The shaded peaks are attributed to the B19 phase. The intensity of the R-phase reflections at room temperature are seen to increase with cooling rate.

Annealing of NiTi at 500° C has been reported to produce excellent shape memory characteristics. Miyazaki *et al.* [7] noted that ageing at 400° C after a solution heat treatment at 1000° C of a 50.6 at % Ni–Ti alloy produced excellent pseudo-elastic behaviour. They also noted improved pseudo-elastic characteristics and increased transformation temperatures in slowly cooled specimens. They considered this to be due to fine precipitates formed by an ageing at 400° C which increase the flow stress for slip. In 49.8 and 50.1 at % Ni–Ti undergoing similar heat treatments, no ageing effects were observed. However, in specimens cold-worked and then annealed at 400° C for 1 h, the lowering of M_s was observed.

49.8 at % Ni–Ti was found to be susceptible to thermal cycling for aged specimens (400° C, 1 h) while in Ni > 50.6 at %–Ti, this was not observed [5]. By annealing at 400° C after cold-work, thermal cycling effects such as the lowering of M_s and M_f and an increase in $(M_s - M_f)$ were not observed, suggesting that either thermally stabilized dislocations retard this effect or that the dislocation density after cold work is sufficiently high that thermal cycling has a negligible effect. The recrystallization temperature is > 400° C [8], hence dislocations are not annealed out. TEM analysis reveals dislocations created with every thermal cycle, as well as R-phase diffraction spots. With increasing dislocation density, M_s decreases and the R-phase temperature remains the same for 49.8 at % Ni–Ti. Diffraction spots are observed to be sharper in 49.8 at % Ni–Ti alloys after a 400° C anneal [9], indicating that the effect may be to reorder the dislocation structure and rearrange their positions to relieve stress.

The purpose of the present work was to investigate the effects on SME performance of ageing effects attributable to R-phase in NiTi and to investigate the physics of these effects.

2. Sample preparation

NiTi, 1.7 mm diameter, was manufactured by Imperial Metals Industries (Kynoch) by a series of hot rolls at 900° C to reduce the wire to 5 mm diameter. After descaling and pickling to remove surface defects, the wire was reduced to 1.5 mm by a series of cold-swages followed by annealing at 900° C and descaling and pickling. It was then wound on to a mandril and held wound at 650° C for 5 min in order to change the preferred cold shape to that of a helical spring suitable for axial deformation tests. Electron microprobe analysis gave the composition as 49.9 at % Ni–Ti. No elemental impurities larger than sodium were detected; however, elements lighter than sodium are not detectable by this method.

The helix was of 1.75 cm diameter with a wire diameter of 1.70 mm, with turns 0.85 cm apart, giving a helix angle of 15.0°. Annealing times and temperatures were 60 ± 5 min at 510 ± 10° C. The spring was packed in alumina powder during the anneal and either remained packed during air cooling or furnace cooling or removed and quenched into 10° C water. A range of several orders of magnitude in cooling rate was thereby achieved.

Samples for DSC analysis were spark cut from the helix and were polished to 1.0 μm, followed by electropolishing in a 5% H_2SO_4, 95% methanol solution (by volume) and finally a chemical etch in 10% HF, 40% HNO_3 and 50% H_2O by volume. Annealing occurred *in situ* in the calorimeter.

3. Crystallographic evidence of a rhombohedral phase

In Fig. 1 are shown the CuK_α X-ray diffraction patterns from a polished section of a helix of polycrystalline NiTi taken at three different cooling rates. The twin peaks at 0.212 and 0.214 nm, seen in the air-cooled and quenched cases, are not associated in either B2 or B19 lattices and are attributed to (1 1 0) lattice plan reflections from a rhombohedral lattice. This R-phase diffraction was also observed by Ling and Kaplow [10]. The rhombohedron must clearly be distorted because there are two peaks which then coincide with two different face diagonals.

The samples were heated to 500° C and then cooled to room temperature for X-ray diffraction studies. When normalized to the intensity of a B19 peak, the

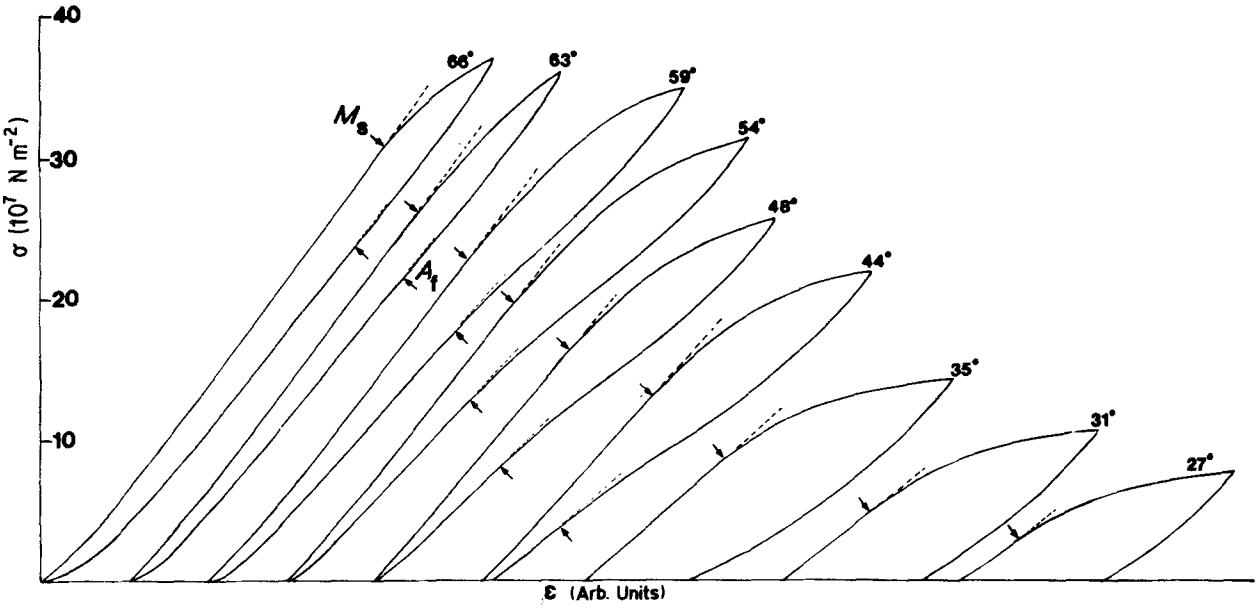

Figure 2 Typical pseudoelastic stress–strain curves for a furnace-cooled NiTi spring. The arrows indicate the $M_s(\sigma_c)$ and $A_f(\sigma_c)$ temperatures. The number at the top of the loops denote the isothermal bath temperature (° C).

ratio of R/B19 is seen to be clearly dependent on cooling rate. The cooling rate from a second anneal at 500° C influences the transformation temperatures of stoichiometric NiTi; the faster the rate of cooling the lower the transformation temperatures. This phenomenon is reversible, i.e. it is solely influenced by the cooling rate from the last 500° C anneal. The relationship between R/B19 and cooling rate can be ascribed to the temperature at which the X-ray data were recorded. From Fig. 1, it is evident that only in the slow-cooled case is the transformation complete, hence no R-phase is observed. As the cooling rate increases, the transformation to martensite becomes less complete and it is here that the R-phase becomes a prominent feature of the diffraction spectrum. The fast-cooled case shows more R-phase than the medium-cooled case.

The influence of cooling rates on transformation temperatures provides a means whereby Carnot efficiencies of SME devices might be influenced. Stress–strain data of NiTi helices cooled from a 500° C anneal by water quenching, air cooling and furnace cooling were analysed and estimates made for the Carnot efficiency.

4. Tensile test results

Tensile tests on the spring were carried out using an Instron Model 1195 tensometer. The specimen was gripped at each end by stainless steel cable secured twice to the outer coils and was further secured by epoxy adhesive.

The sample was heated in a water bath contained in a 2 litre water-tight can mounted in the tensometer. Frequent stirrings ensured a reasonably even temperature throughout. Ten loading–unloading tensile tests were performed at different temperatures to determine the variation of M_s and A_f with temperature.

A sequence of stress–strain curves is shown in Fig. 2. The initial slope is the Young's modulus of the bulk austenitic (B2) phase, the gradual shift to a new straight line being due to the formation of the stress-induced martensite. In single crystal specimens the transformation is more abrupt; in polycrystalline specimens the stress–strain curve represents an average of the transformation curves for all the grains in the specimen, hence a gradual transformation. Similarly on unloading, the change in slope is due to the retransformation of stress-induced martensite back to austenite. Timoshenko [11] analysed the distribution in torsional stress in a cross-section of the wire of a helix when subjected to axial loading. The maximum stress the wire experiences is given by

$$\sigma_{max} = 16FR(1 + \sin \alpha)/\pi d^3 \quad (1)$$

where F is the axial load, R is the mean radius of the spring, d is the diameter of the wire and α is the pitch angle of the spring. The regions subjected to maximum stress are the first to transform, and the maximum stress can be easily determined as where the load–extension curve first deviates from the straight line defined by the initial elastic behaviour of the austenite in either the loading or unloading case.

The temperature of the bath was determined using a mercury thermometer held adjacent to the spring. Readings were noted at three points; the beginning, the end and the midpoint of the loading cycle. The temperature at the M_s and A_f point was determined by linear interpolation.

The critical stress (σ_c) required to induce a martensitic transformation, was measured to determine the Carnot efficiencies for the various cooling rates. At temperatures greater than 70° C, the spring was loaded until the yield point was detected. The increase of the width in hysteresis loop compared with those for less loaded high-temperature curves confirms that plastic deformation had taken place. The stress at which the yield point occurred (σ_{max}) was calculated using Equation 1. It was observed that σ_c was not significantly affected by differing cooling rates.

The transformation temperatures M_s and A_f are plotted against stress for the three cooling cases in

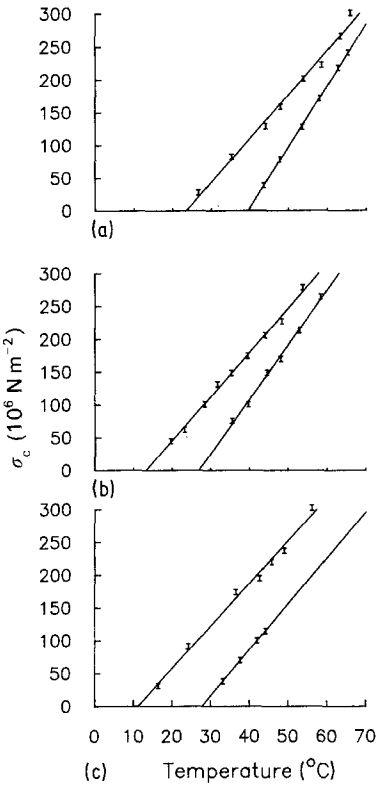

Figure 3 M_s and A_f temperature dependence on critical stress (σ_c) for three cooling rates from a 500° C anneal. The left-hand line describes B2 → B19 transformation with stress, the right-hand line describes the reverse transformation. (a) Furnace cooled: $M_s = 1.49 \times 10^{-7}\sigma_c + 24.6°\,C$ and $A_f = 1.08 \times 10^{-7}\sigma_c + 39.6°\,C$. (b) Air cooled: $M_s = 1.47 \times 10^{-7}\sigma_c + 13.9°\,C$ and $A_f = 1.22 \times 10^{-7}\sigma_c + 26.9°\,C$. (c) Quenched: $M_s = 1.53 \times 10^{-7}\sigma_c + 12.3°\,C$ and $A_f = 1.60 \times 10^{-7}\sigma_c + 29.0°\,C$.

Figs 3a to c. The equation relating transformation temperature to stress is of the form

$$M_s = (dM_s/d\sigma_c)\sigma_c + M_s(\sigma_c = 0) \quad (2)$$

or

$$A_f = (dA_f/d\sigma_c)\sigma_c + A_f(\sigma_c = 0)$$

A least squares analysis of the data gave the following straight lines.

Furnace cooled

$$M_s = 1.49 \pm 0.07 \times 10^{-7}\sigma_c + 23.7 \pm 0.14°\,C$$
$$A_f = 1.07 \pm 0.03 \times 10^{-7}\sigma_c + 39.4 \pm 0.6°\,C \quad (3)$$

Air cooled

$$M_s = 1.47 \pm 0.05 \times 10^{-7}\sigma_c + 13.8 \pm 1.0°\,C$$
$$A_f = 1.22 \pm 0.11 \times 10^{-7}\sigma_c + 26.7 \pm 2.2°\,C$$

Quenched

$$M_s = 1.53 \pm 0.06 \times 10^{-7}\sigma_c + 12.2 \pm 1.2°\,C$$
$$A_f = 1.60 \pm 0.06 \times 10^{-7}\sigma_c + 26.8 \pm 0.6°\,C$$

The Carnot efficiency of SME alloy heat engines is [12]

$$\eta_c = 1 - \frac{M_f(\sigma \to 0)}{A_f(\sigma \to 0) + \sigma_{max}(dA_f/d\sigma_c)} \quad (4)$$

where $M_s(\sigma \to 0)$ and $A_f(\sigma \to 0)$ refer to the transformation temperatures as stress vanishes, σ_{max} is the maximum stress which can be applied before plastic deformation and $dA_f/d\sigma_c$ is the gradient of A_f with critical stress (σ_c). The Carnot efficiencies for the three cooling rates are calculated using Equation 4

Furnace cooled $\eta_c = 0.136 \pm 0.012$ (5a)

Air cooled $\eta_c = 0.149 \pm 0.022$ (5b)

Quenched $\eta_c = 0.164 \pm 0.014$ (5c)

It is also likely that the thermal efficiency of NiTi heat engines will increase with increased cooling rate of the NiTi working substance from a high-temperature anneal. This can be seen in Figs 3a to c. The quenched cooling rate gives rise to an increased hysteresis as the A_f–σ_c line becomes progressively more parallel to the M_s–σ_c line. It is interesting that $dM_s/d\sigma_c$ does not change with cooling rate within experimental error.

5. Ageing effects

In order to establish why the thermodynamic data change with cooling rate, ageing experiments at 400 and 450° C were performed with small samples of the spring which were mechanically cut and annealed at 500° C for 1 h followed by quenching. A Perkin–Elmer differential scanning calorimeter (DSC-2) was used to measure the transformation temperatures and latent heats. The specimens could be heated to test temperature in about 1.5 min and could be cooled at a controlled rate of up to 320° C min^{-1}. As the DSC had no sub-ambient temperature control, controlled cooling could only be obtained down to 25° C. The samples were removed at room temperature and placed in a freezer at −5° C to ensure a "complete" martensitic transformation. From observing the shape restoration of deformed helices in a thermal cycling rig, rapidly cooled NiTi began shape restoration at 4° C, and in slowly cooled NiTi at 43° C. Latent heat experiments at 5° C min^{-1} for heating and 2.5° C min^{-1} for cooling were performed. To calibrate the latent heat measurements, the melting of an indium standard sample was measured.

Characteristic latent heat curves for first-order transformations are roughly "saw-toothed" in profile. A_s is determined from the start of the slope of the saw-tooth, and A_f is measured from where the peak is at a maximum. The measurement of the latent heat of the transformation is taken as the area contained under the curve and above the baseline. An initial starting transient is observed when heating or cooling commences; the height of the transient from an isothermal baseline is a measure of the specific heat of the sample. These transients are included with the latent heat curves obtained during heating as shown in Figs 4 and 5.

As ageing time increases at 400° C (Fig. 4), the temperature for the martensite–austenite transition increases. Also, a small latent heat peak occurs at a slightly lower temperature, which is more evident with increased ageing. At low annealing times the peaks display a small amount of asymmetry, which increases at intermediate annealing times. As the "pre-austentic"

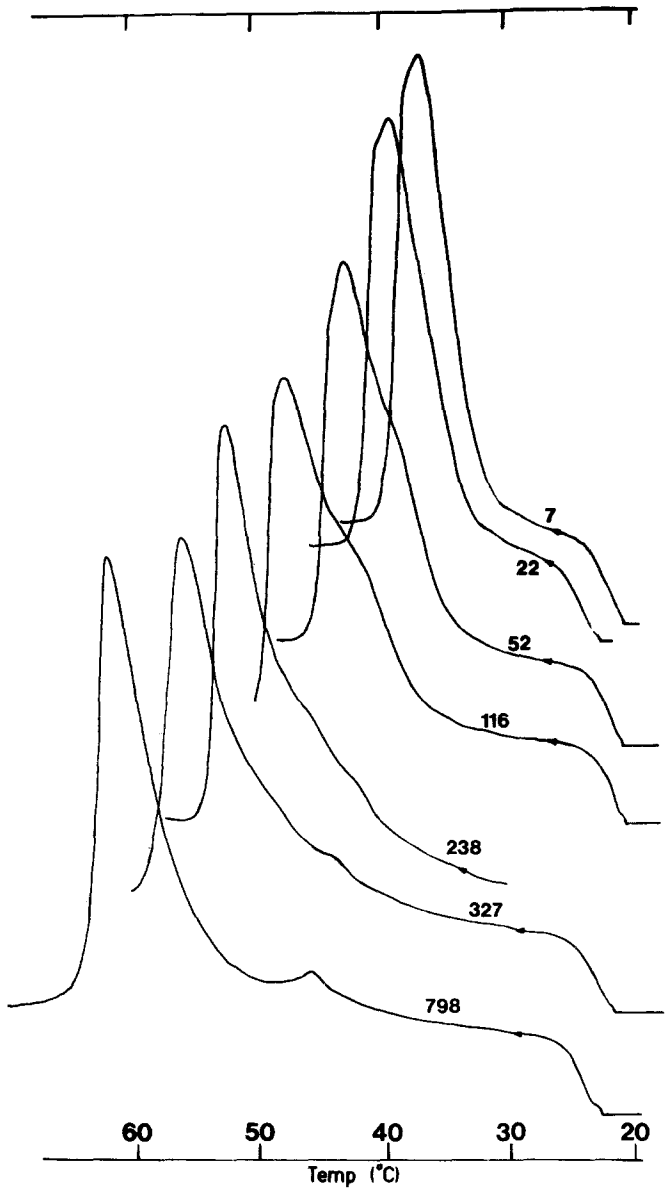

Figure 4 Endotherms for the anneal at 400° C. Figures refer to ageing time in minutes. Note the appearance of a secondary peak which evolves with increased ageing time.

peak diverges, the major austenitic peak becomes narrower.

Annealing at 450° C reveals dramatic trends (Fig. 5). Initially the austenitic latent heat peak was broad but after 5 min at temperature, it narrowed considerably. The large austenitic peak maintains a reasonably constant profile once ageing begins. Increasing ageing reveals a concomitant increase in A_s and A_f. A small additional latent heat peak is observed after ageing between 5 and 20 min. The area of the small peak as well as the temperature at which it occurs (designated R) is seen to increase with ageing. This peak also broadens with ageing.

Cooling produced the curves shown in Fig. 6. A small secondary peak is also observed on the main peak, which maintains its position with respect to the major peak during ageing. It probably originates from a less stressed region of the sample that would then transform at a lower temperature. The exothermic peak increases in magnitude as does the temperature at which it starts with ageing.

The secondary latent heat peaks obscure some A_s values (Fig. 4), and do not follow the same ageing behaviour as the main B19 → B2 peak. The temperature of the secondary peak was determined as the maximum deviation from the major peak slope. The transition temperature for this peak varies with ageing and could be linearly extrapolated to the finishing temperature of the small latent heat peaks. It is reasonable to assume that the secondary peaks are due to this second transformation.

The transformation temperature for the two annealing temperatures are plotted in Figs 7 and 8. Both A_s and A_f are non-linear with ageing time at 450 or 400° C. The small secondary peak follows a different linear curve at 450° C suggesting that this peak is not martensitic in nature.

6. Temperature cycling experiments

Temperature cycling experiments on material aged at 450° C for long times also reveal remarkable properties. Fig. 9 shows the results of a heating → cooling → heating → cooling cycle performed on a specimen aged for 1083 min. The specimen was initially cooled in a freezer to − 5° C so that the martensitic transformation was complete and then heated in the DSC, producing the endotherm as seen in Fig. 9a. Subsequent cooling produced the exotherm (Fig. 9b) from which it was judged that the transformation had been completed. Heating from this temperature produces a

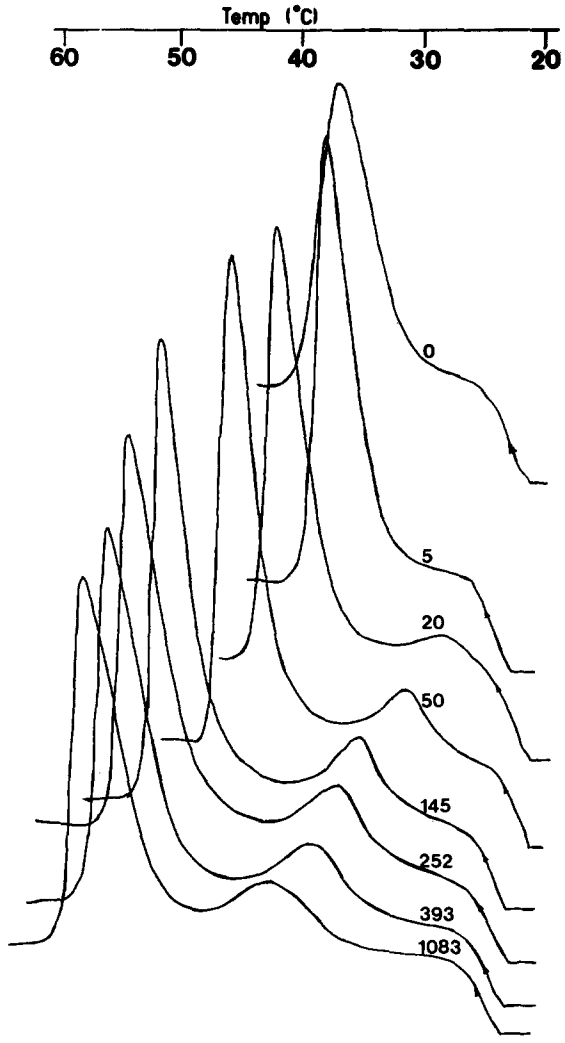

Figure 5 Endotherms for the anneal at 450° C. Figures refer to ageing times in minutes. Note the appearance of a pre-austenitic peak with increasing ageing time.

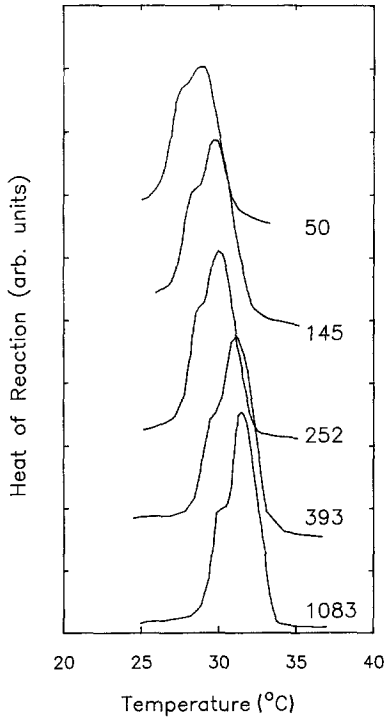

Figure 6 Exotherms observed on cooling from a fully austenitic structure for various ageing times at 450° C. Numbers on the right indicate ageing time in minutes.

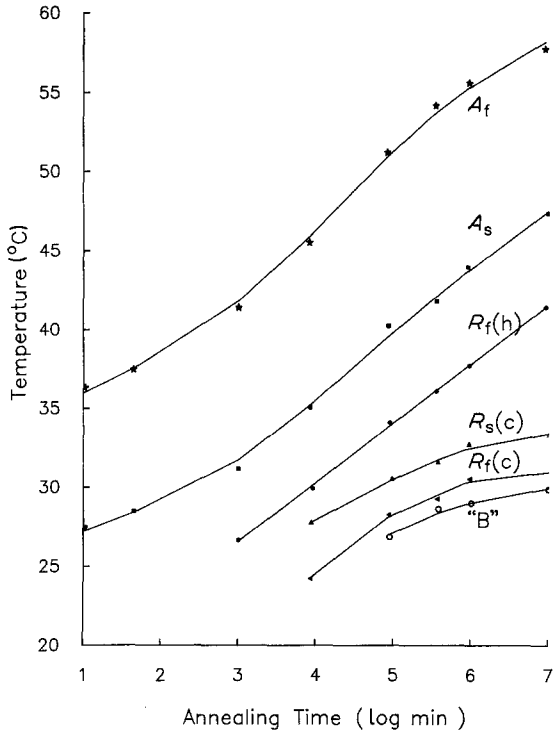

Figure 7 Transformation temperatures plotted against ageing time at 450° C. Both A_s, A_f are nonlinear. R_f is linear with heating. The B2 → R transformation is also affected by ageing. B refers to a small peak which is seen on the large exothermic peak. It is considered to be due to a region where R transforms at a different temperature, but has the same ageing characteristics.

large endothermic peak at about 5° C above the temperature of exothermic reaction (Fig. 9c), as well as a small peak where the B19 → B2 transformation occurs. Cooling again, Fig. 9d, shows the same behaviour as in Fig. 9b, indicating that the reaction is reversible. This experiment was repeated for three different annealing times and showed similar behaviour each time.

These observations support the notion that the cooling peaks and the small endothermic peaks observed on heating are associated with the R-phase. Transformation to and from the R-phase reveals a hysteresis of approximately 5° C. The R → B2 transformation occurs at higher temperatures with ageing. There is also an ageing effect on the temperature of the reverse transformation, B2 → R (Fig. 7). The latent heats involved during heating and cooling are different, as expected, because in one case, R → B2 and in the other case R → B19. The small latent heat bump observed at A_f in Fig. 9c is attributed to a small fraction of B19 formed during the cooling stage.

7. Latent heat measurements

The endothermic latent heats for the two annealing temperatures are shown plotted against the logarithm of annealing time in Figs 10 and 11. In both cases the measured latent heats of the austenite to martensite transformation are reasonably constant with ageing, which indicates that there is no change in the volume fraction of material transforming martensitically. The intial latent heat values are somewhat different, which may be attributable to a defective volume fraction not having been annealed out before testing. It would

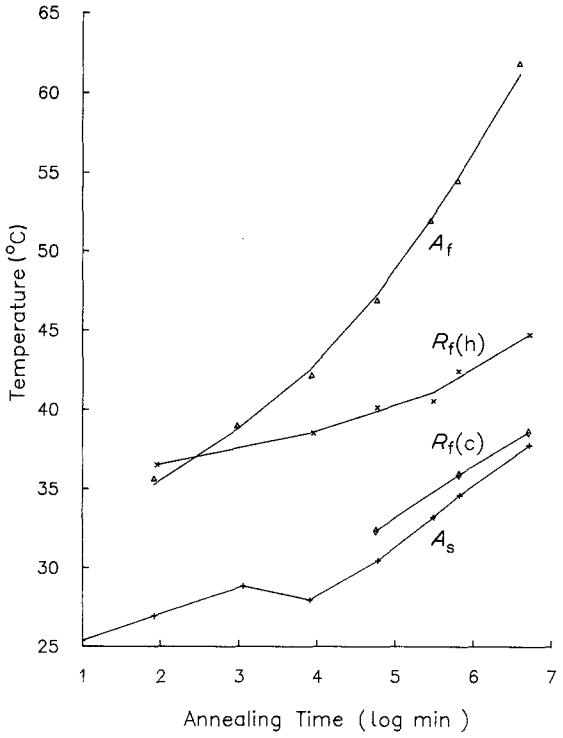

Figure 8 Transformation temperatures plotted against ageing time at 400° C. The A_s curve has a kink in it which may be due to the formation of the R-phase.

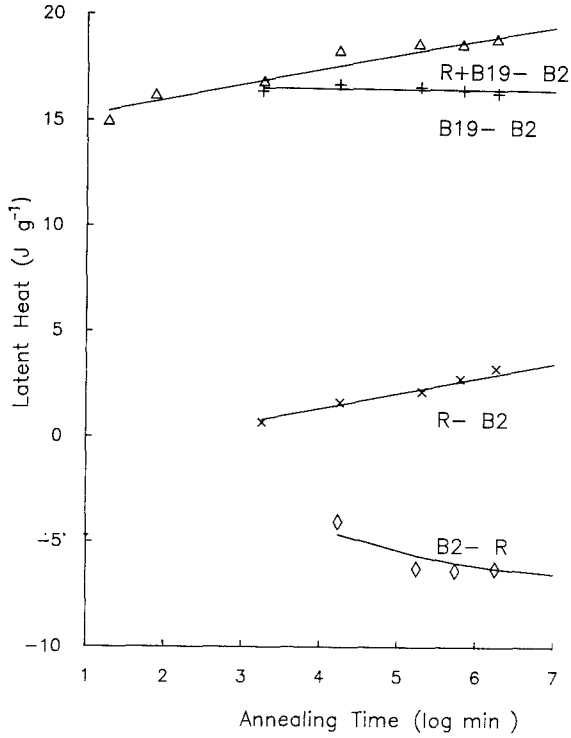

Figure 10 Variation with ageing times at 450° C of latent heat measurements of the various transformations present. The latent heat for B + B19 → B2 transformation remains constant after 20 min suggesting that the R increase cannot be due to material transformation to R without transforming to B2.

appear that the secondary peak corresponds to a non-martensitic transformation which does not affect the austenitic transformation.

The endothermic latent heat measurements at 400° C (Fig. 10) show that the latent heat increases with ageing. This is not the case at 450° C where the heat evolved is constant throughout the annealing time range (Fig. 11). An increasing latent heat indicates more material is transforming as ageing continues, which is not in character with a martensitic transformation. Presumably the lack of dependence of latent heat on ageing at 450° C indicates that all the material that could transform has done so after 50 min ageing.

A final experiment was performed on the specimen aged at 400° C. After a latent heat trace was obtained (Fig. 12a), it was placed in a furnace at 510° C for 1 h and then furnace-cooled. DSC analysis shows one

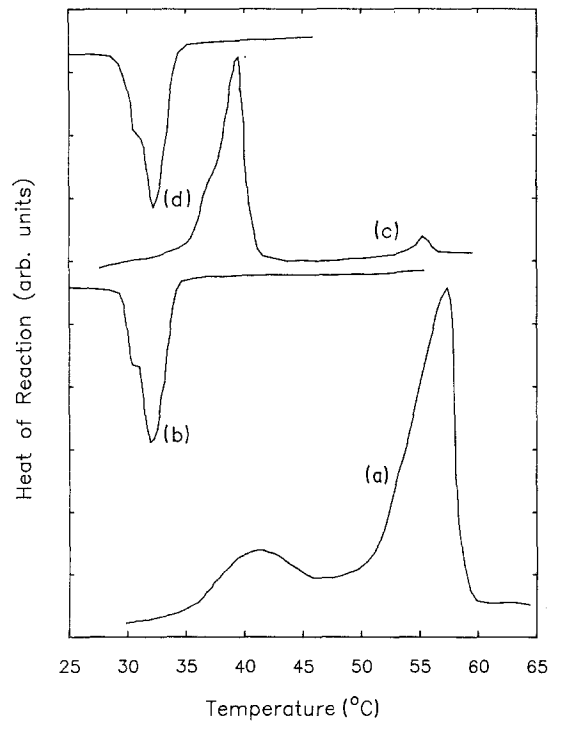

Figure 9 DSC scans. (a) Heating from a fully completed martensitic reaction produces a latent heat for B19 → R and B19 → B2. (b) Cooling produces a large exothermic peak. (c) Subsequent reheating produces peaks corresponding to B19 → R at a different temperature. The peak for B19 → R remains at the same temperature, though diminished. (d) Cooling again produces the same exotherm as in (b), indicating that this peak is B2 → R.

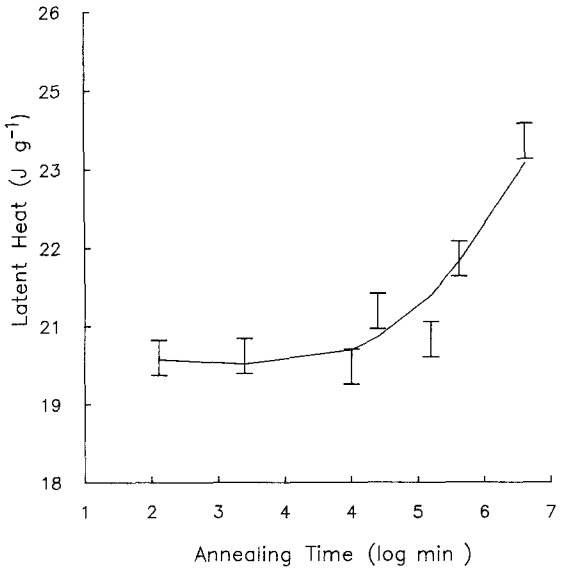

Figure 11 Endothermic latent heat of the peak observed with ageing at 400° C. The increase in value is attributed to the formation of R at longer annealing times.

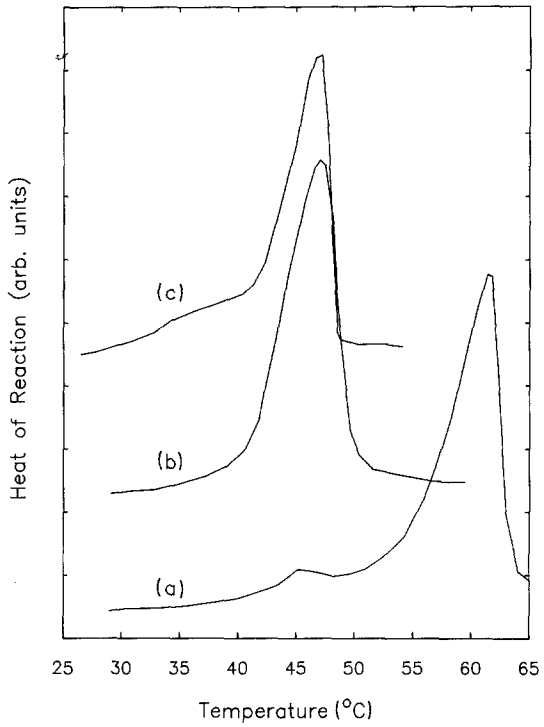

Figure 12 Influence of 500° C heat treatment on ageing effects. (a) Endotherm for specimen given 13 h anneal at 400° C. (b) Same as specimen (a) after a 500° C anneal plus furnace cooling. (c) Endotherm for a similar sample after 500° C anneal plus furnace cooling. 500° C heat treatment nullifies the ageing effects seen after 400 and 450° C anneals.

broad peak at 323 K (Fig. 12b), indicating that whatever is responsible for these two effects, it is destroyed by ageing at 500° C for 60 min. The cooling curve of the furnace is such that the dwell time at 450° C is 20 min and at 400° C it is 1 h. Another sample was cut from the same spring and subjected to the same conditions as the annealed spring (Fig. 12c). Although broader in peak width, the transformation temperatures were the same. Neither sample exhibited an increase in transformation temperature after the anneal at 500° C, indicating that both effects must be related to a mechanism(s) which is destroyed at temperatures above approximately 500° C.

8. Discussion

It has been demonstrated that ageing at 400 and 450° C results in:

(a) separation and enhancement of a second transformation whereas after an anneal at 500° C followed by quenching, this transformation is not observed on heating;

(b) the increase in latent heats with ageing at 400° C suggests that an increasing volume of crystal undergoes this second transformation;

(c) increasing austenitic transformation temperatures is observed with continued ageing.

(d) The martensitic (B19 → B2) transformation follows a different type of temperature–time behaviour than does the secondary transformation.

What is the nature of this secondary peak and what is the physical cause of the ageing effects? Referring first to the pseudo-elasticity behaviour and efficiencies discussed, the slower the cooling rate and the longer the ageing time at 450 and 400° C, the higher the transformation temperatures and the larger the amount of material transforming to the intermediate R-phase.

It is interesting that in the cooling experiments the $dM_s/d\sigma_c$ values were not affected by cooling rate, whereas the $dA_f/d\sigma_c$ are. This results in an increased hysteresis at high cooling rates. The $dM_s/d\sigma_c$ values for three different cooling rates can be explained as a difference in pre-stresses in the crystal, so that the $dM_s/d\sigma_c$ values are translated up or down in temperature without a change in slope. This is not true for $dA_f/d\sigma_c$ where a change in slope as well as a change in pre-stressing occurs.

The secondary transformation observed on heating is probably R → B2 as this process has an entirely different behaviour to the B2 → B19 transformations. Goo and Sinclair [3] point out that the R-phase is not a premartensitic precursor but an entirely separate transformation. Separation of the R-phase from the martensitic transformations is also consistent with annealing after cold work. What makes these observations interesting is that R → B2 has been observed, which has not been reported previously.

Assuming that the increase in A_s, A_f and R with ageing are due to stress by some mechanism, it is interesting that the R → B2 transformation is stress-dependent. A Clapeyron relationship has been measured for R → B19 [9] which shows a steeper slope than for B2 → B19. There is a slight volume increase which makes this transformation stress-dependent.

We have also observed a complete cycle of R →← B2 (Figs. 9b, c). Ling and Kaplow [10] reported that in two-way memory NiTi, the R-phase was observed to contribute by as much as one-third to the overall shape-change of the specimen on cooling. Computer simulations of the R-phase formation by Jardine [14] based upon lattice displacement wave observations by Sinclair and co-worker [15–17] show that the B2 → R transformation does comply with the perfect SME criterion that "one principal stress be equal to zero". This raises the interesting possibility of cycling the NiTi so that only the R-phase formation occurred, thus giving the advantage of perfect shape-memory, but with the disadvantage of a much reduced thermal efficiency.

The microstructure of the specimens was examined to see if ageing had affected the gross features of the system. A comparison of optical micrographs taken of a sample annealed at 500° C and quenched compared to one annealed at 450° C for 1 h and then slowly cooled showed no discernable differences. None was expected, as the recrystallization temperature is 650° C. Nishida *et al.* [8] have also observed no change in microstructure between quenched and furnace-cooled Ni–Ti from an anneal at 1000° C. Further, no secondary phase appears.

The increase in overall transformation cannot be due to precipitation as the near-stoichiometric composition of the alloy rules out the precipitation of nickel- or titanium-rich precipitates.

A systematic error in the experiment, such as incomplete transformations generating dislocations, is

a possibility. However, the recrystallization temperature is far greater than 500° C so that dislocations created by incomplete cycling should not be lost, and so at 500° C the ageing effect should continue. The role of dislocations introduced to a far larger extent by cold-working in the creation of the helix, or a possible ordering transformation, or both, must be considered.

The behaviour of the amount of R-phase with ageing temperature is similar to an order–disorder transformation occurring near 450° C. It is clear that ageing at 450° C is more effective than at 400° C, whereas at 500° C the R-phase enhancement disappears.

Wang and Buehler [18] have reported an order–disorder transformation in NiTi occurring between 650 and 700° C when a disordered b c c structure transforms to a complex CsCl-type B2 structure. The effect of atomic order on martensitic transformations has been the subject of considerable study (Ling and Owen [19]), although there have been no reported ordering studies on NiTi. Studies of Fe_3Pt and CuAlNi show that increased ordering of lattice sites promotes higher transformation temperatures. It is reasonable to expect that ordering produces similar effects in NiTi.

A DSC scan was taken between 200 and 500° C and no latent heat anomalies were observed, thus indicating that either the transformation is not first order or that ordering involves a small number of components so that the latent heat is not resolvable. The order–disorder transformation occurring near 400° C could involve ordering of impurities and/or vacancies in the structures. As an example of this, Moine *et al.* [20] found that, in thin foils of Ti–50.5 at % Ni heated in an electron microscope *in situ*, odd surface effects in the thin foil were observed and the martensitic transformation was suppresed below −198° C, unlike in bulk specimens which did transform at higher temperatures. They considered that this was possibly due to contamination of the thin foil with oxygen atoms during annealing coupled with a possible ordering of the interstitial oxygen atoms or vacancies within the specimen.

Dislocations introduced by cold-working must be a part of the effect, as the straight wire showed no ageing effects. However, annealing at 500° C removes this effect, but does not remove any dislocations. The mobility of dislocations around defects and how they redistribute themselves to accommodate stress may be important. Creation of dislocations on annealing at 400° C after cold-work in 49.8 at % Ni–Ti and 50.6 at % Ni–Ti has been observed [9]. Sharp diffraction spots were seen after ageing, ascribed to the rearrangement of dislocations to relieve strains. At 500° C, the dislocations may be sufficiently mobile to leave the nucleation sites and so the effect is lost.

9. Conclusions

1. The enhanced pseudo-elastic characteristics for near-stoichiometric specimens annealed at 500° C are attributed to the formation of rhombohedral distortions which enhance the transformation.

2. Ageing at 450° C promotes more material transforming to the R-phase with no change in amount of material transforming martensitically. This is expected to enhance the SME by providing additional latent heat and shape recovery characteristics.

3. It should be possible to exploit R-phase transformation to generate perfect shape memory albeit with loss of Carnot efficiency and thermal efficiency.

Acknowledgements

APJ thanks the British Gas plc for a scholarship. We also acknowledge helpful discussions with Dr R. Stevens of British Gas and specimen preparation assistance from Mr M. L. Gabb and Mr H. N. Young of Bristol University.

References

1. F. E. WANG, W. J. BUEHLER and S. J. PICKART, *J. Appl. Phys.* **36** (1965) 3232.
2. M. UMEMOTO and C. M. WAYMAN, *Metall. Trans.* **A9** (1978) 891.
3. T. SUBURI, T. TATSUMI and S. NENNO, Proc. ICOMAT (Leuven), *J. de Phys.* **43** (1982) C4-261.
4. G. D. SANDROCK, A. J. PERKINS and R. F. HEHEMANN, *Metall. Trans.* **12** (1971) 2769.
5. S. MIYAZAKI, Y. IGO and K. OTSUKA, *Acta Metall.* **34** (1986) 2045.
6. V. I. KHACHIN, Y. I. PASKAL, V. E. GUNTER, A. A. MONASEVICH and V. P. SIVOKHA, *Phys. Metal. Metallogr.* **46** (1978) 49.
7. S. MIYAZAKI, Y. OHMI, K. OTSUKA and Y. SUZUKI, Proc. ICOMAT (Leuven), *J. de Phys.* **43** (1982) C4-255.
8. M. NISHIDA, C. M. WAYMAN and T. HONMA, *Metall. Trans. A* **17A** (1986) 1505.
9. S. MIYAZAKI and K. OTSUKA, *ibid.* **17A** (1986) 53.
10. H. C. LING and R. KAPLOW, *ibid.* **11A** (1980) 77.
11. S. TIMOSHENKO, "Strength of Materials", Vol. II (Van Nostrand, Princeton, N.J., 1956) p. 304
12. B. CUNNINGHAM and K. H. G. ASHBEE, *Acta Metall.* **25** (1977) 1315.
13. E. GOO and R. SINCLAIR, *ibid.* **33** (1985) 1717.
14. A. P. JARDINE, PhD thesis, Bristol University (1986) p. 75.
15. P. MOINE, G. M. MICHAL and R. SINCLAIR, *Acta Metall.* **30** (1982) 109.
16. G. M. MICHAL, P. MOINE and R. SINCLAIR, *ibid.* **30** (1982) 125.
17. P. MOINE, E. GOO and R. SINCLAIR, *Scripta Metall.* **18** (1984) 1147.
18. F. E. WANG and W. J. BUEHLER, *Appl. Phys. Lett.* **21** (1972) 105.
19. H. C. LING and W. S. OWEN, *Acta Metall.* **29** (1981) 1721.
20. P. MOINE, E. GOO and R. SINCLAIR, ICOMAT (Leuven), *J. de Phys.* **43** (1982) C4-243.

Received 10 November 1987
and accepted 3 March 1988